Toxicology Reports 2 (2015) 1213–1221

Contents lists available at ScienceDirect

Toxicology Reports

journal homepage: www.elsevier.com/locate/toxrep

Protective effect of *p*-coumaric acid against doxorubicin induced toxicity in H9c2 cardiomyoblast cell lines

Sunitha M. Chacko [1], Kottayath G. Nevin [*,1], R. Dhanyakrishnan, B.Prakash Kumar

School of Biosciences, Mahatma Gandhi University, PD Hills PO, Kottayam, Kerala 686560, India

ARTICLE INFO

Article history:
Received 2 May 2015
Received in revised form 23 July 2015
Accepted 6 August 2015
Available online 10 August 2015

Keywords:
p-Coumaric acid
Doxorubicin
H9c2 cells
ROS
Cytotoxicity

ABSTRACT

Doxorubicin (Dox) has been used for more than four decades to treat cancer, particularly solid tumours and haematological malignancies. However, the administration of this drug is a matter of concern in the clinical community, since Dox therapy is commonly associated with dose-dependent cardiotoxicity. Attempts at alleviating drug generated cardiac damage using naturally occurring compounds with radical scavenging property are a promising area of research. *p*-Coumaric acid (*p*CA) is one such compound which has significant antiradical scavenging effect. This study aims to investigate the effect of pre and co-administration of *p*CA on mitigating or preventing Dox induced cardiotoxicity *in vitro* using H9c2 cardiomyoblast cell lines. Addition of *p*CA and Dox were performed for both treatment and control sets on H9c2 cells. Sulphorhodamine B assay was used to study the cytotoxic effect of *p*CA and Dox. The effect of the drug on cell morphology, cell viability and nuclear damage was studied using AO/EB and DAPI staining. ROS production was studied using DCFH-DA staining. Mitochondrial membrane potential and intracellular calcium levels were assessed by rhodamine 123 and Fura 2AM staining. *p*CA showed strong ABTS cation radical scavenging activity and FRAP activity in a dose dependent manner. The results showed that Dox has significant cytotoxic effect in a dose dependent manner while *p*CA, even at higher concentrations did not display any significant cytotoxicity on H9c2 cells. Both pre treatment and co-administration of *p*CA reduced the drug induced toxic effects on cell morphology and enhanced the number of viable cells in comparison to the Dox treated cells as evident from the AO/EB and DAPI staining images. The Dox induced ROS production was found to be significantly reduced in *p*CA pre-treated and co-administered cells. Dox induced changes in mitochondrial membrane potential and intracellular calcium levels were remarkably improved following pre and co-treatment of H9c2 cells with pCA. These results clearly suggest that pre-treatment and co-administration of *p*CA is a promising therapeutic intervention in managing Dox mediated cardiotoxicity.

1. Introduction

Doxorubicin (Dox) is an anthracycline antibiotic effective in the treatment of solid tumours and *haematological* malignancies [1]. This drug is commonly used as part of a combination regimen in both paediatric and adult patients. However, administration of Dox is a matter of concern in the clinical community since anthracycline therapy is commonly associated with dose-dependent cardiotoxicity [2]. Though the exact mechanism of cardiotoxicity is not yet fully understood, Dox evidently induced membrane alterations through lipid peroxidation, free radical generation, increased myocardial levesl of sodium and calcium, impaired myocardial DNA and RNA synthesis and induced apoptosis on cardiomyocytes [3–6]. Drug induced toxicity is a multifactorial process and one of the most common causes attributed to this is the generation of reactive oxygen species (ROS)/nitrogen species (RNS) as a result of drug redox recycling. It has therefore been suggested that some phytochemicals with high antioxidant potential, when administered together with antitumour agents, could decrease/attenuate the toxic side effects of chemotherapy induced as a byproduct of oxidative stress and thus reduce the risk of heart failure [7]. Attempts are progressing to alleviate drug generated ROS induced damage, using naturally occurring compounds with radical scavenging property. Naturally

Abbreviations: DMEM, Dulbecco's modified Eagle's medium; FBS, foetal bovine serum; DAPI, trypan blue, 4′,6-diamidino-2-phenylindole; *p*CA, *p*-coumaric acid; SRB, sulphorhodamine-B; DCFH-DA, dichlorofluorescin diacetate; ROS, reactive oxygen species; Dox, doxorubicin; ABTS, 2,2′-azinobis-(3-ethylbenzothiazoline-6-sulfonic acid); RNS, reactive nitrogen species.

* Corresponding author.
E-mail address: nevinkg@gmail.com (K.G. Nevin).
[1] Both the authors contributed equally to this work.

http://dx.doi.org/10.1016/j.toxrep.2015.08.002

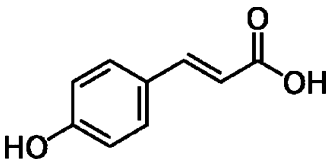

Fig. 1. Chemical structure of *p*-coumaric acid [3-(4-hydroxyphenyl)-2-propenoic acid].

occurring antioxidant compounds such as naringenin, probucol, resveratrol, epigallocatechin gallate and quercetin have been tried and tested with promising results with regards to their effect on Dox induced toxicity in *in vitro* studies as well as in animal models [8–12]. *p*-Coumaric acid (*p*CA), a hydroxy derivative of cinnamic acid (Fig. 1) can be found in a wide variety of edible plants such as peanuts, barley grains, navy beans, tomatoes, carrots, garlic and honey. It is also present in wine and vinegar in significant amounts [13–15]. *p*CA is one of the many phenolic compounds which is consumed on a daily basis by a majority of the population worldwide through their routine dietary intake. *p*CA is also reported to have antioxidant properties and is believed to reduce the risk of stomach cancer by reducing the formation of carcinogenic nitrosamines [16,17]. Though *p*CA possess anticancer activity, the cardioprotective effect of the phenol has not been studied progressively. This study was designed to evaluate the beneficial effect of *p*CA on Dox induced toxicity in rat-derived cardiomyoblast cell lines in *in vitro* conditions.

2. Materials and methods

2.1. Chemicals

Dulbecco's modified Eagle's medium (DMEM), foetal bovine serum (FBS) and other cell culture reagents were procured from Hi-Media Laboratories. Acridine orange (AO), ethidium bromide (EB), trypan blue, 4′,6-diamidino-2-phenylindole dihydrochloride (DAPI) and rhodamine-123(R-123) were obtained from Hi-Media Laboratories, India. Doxorubicin hydrochloride, *p*-coumaric acid, sulphorhodamine-B (SRB), dichlorofluorescin diacetate (DCFH-DA) and 2,2′-azinobis-(3-ethylbenzothiazoline-6-sulfonic acid (ABTS) were purchased from Sigma–Aldrich, USA. Fura-2 acetoxymethyl ester (Fura-2AM) was purchased from Invitrogen.

2.2. ABTS cation free radical-scavenging activity

Free radical scavenging ability of *p*CA in terms of $ABTS^+$ radical scavenging activity was evaluated by the procedure of Re et al. [18], with some minor modifications. ABTS which is a colourless compound is converted to its blue–green counterpart $ABTS^+$ by the loss of an electron by nitrogen on the parent compound. $ABTS^+$ was generated by reacting ABTS stock solution with 2.45 mM potassium persulfate and allowing the mixture to stand in the dark at room temperature for 12–16 h prior to use. Different concentrations of *p*CA (0.04–152 μM) were allowed to react with 180 μL of $ABTS^+$ solution for 12 min under dark conditions at room temperature. The absorbance of the sample was measured at 734 nm. Butylated hydroxyl toluene (BHT) was used as positive control. The activity was expressed as percentage of $ABTS^+$ radical scavenging calculated by the following formula:

$$ABTS^+ \text{scavenging activity}(\%) = [\frac{(A_c - A_t)}{(A_c)} \times 100],$$

where A_c is the absorbance value of the control and A_t is the absorbance value of the test samples.

2.3. Ferric-reducing/antioxidant power (FRAP) assay

The FRAP assay was carried out by the method described by Benzie and Strain [19]. This method is based on the principle of reduction of Fe^{3+}-TPTZ (2,4,6-tripyridyl-s-triazine) to Fe^{2+} TPTZ complex at a low pH which gives purple–blue colour measured at 595 nm. Briefly, different concentrations of *p*CA (0.04–152 μM) was mixed with 180 μL of FRAP reagent (300 mM acetate buffer pH 3.6, 10 mM TPTZ in 40 mM HCl and 20 mM $FeCl_3 \cdot 6H_2O$ in the volume ratio 10:1:1) on a 96 well plate. Mixture was allowed to stand for 6 min and absorbance of samples was measured at 595 nm. Ascorbic acid and $FeSO_4$ were used as reference standards. An increase in absorbance was considered as an indicator of a higher antioxidant potential.

2.4. Cell culture

H9c2 myoblast cells derived from the rat myocardium was obtained from National Centre for Cell Sciences (NCCS), Pune, India. The myoblast cells were cultured in Dulbecco's modified Eagle's Medium (DMEM) medium supplemented with 10% FBS and 10 ml/l 100 × antibiotic–antimycotic solution containing 10,000 units of penicillin and 10 mg/ml streptomycin in 0.9% normal saline in a humidified atmosphere of 95% air and 5% CO_2 at 37 °C.

2.5. Cytotoxicity analysis

Cytotoxicity of different concentrations of *p*CA and Dox was evaluated individually using the sulphorhodamine B assay (SRB). SRB is a bright pink aminoxanthene dye which binds to proteins electrostatically under mildly acidic conditions. The fixed dye, measured photometrically after solubilisation correlates with total protein synthesis rates and thereby with cell proliferation [20]. To determine and standardise the concentration of *p*CA and Dox to be used in further experiments, H9c2 cells (2×10^4 cells/well in 96 well plates) were seeded with DMEM medium and incubated for 48 h at 37 °C with 95% air and 5% CO_2 to allow the cells to become semi confluent (70–80%). Adhered cells were then treated with different concentrations of *p*CA (24–760 μM) and Dox (0.1–13 μM) individually for 72 h. After the experimental period, cell fixation was carried out by the addition of 50% ice-cold trichloroacetic acid (TCA). Plates were then incubated at 4 °C for 30 min and the plates were then rinsed 4-5 times under running tap water. Plates were air-dried and 50 μL of SRB solution (0.4% in 1% acetic acid) was added to each well and incubated for 20 min at room temperature. At the end of the staining period the plates were washed with 1% acetic acid to remove the unbound dye and bound dye was solubilised by the addition of 10 mM Tris base (pH 10.5). Absorbance was measured at 490 nm on a Thermoscientific Varioskan Flash Microplate Reader. IC_{50} values were calculated by plotting the OD readings *versus* the drug concentrations. Percentage cell death was calculated by the following formula.

$$\%\,\text{Cell death} = \frac{OD_{Control} - OD_{Test}}{OD_{Control}} \times 100$$

2.6. Cytotoxicity of pre and co-administration of pCA with Dox

To determine the cytotoxicity and morphological changes during pre and co-administration of *p*CA and Dox, H9c2 cells (2×10^4 cells/well in 96-well plates) were seeded with DMEM medium and incubated for 48 h at 37 °C with 95% air and 5% CO_2 to allow the cells to become semi-confluent. After this period the cells were pre/co-treated with *p*CA (380 μM) and Dox (1.5 Dox μM) respectively, for 72 h. After the incubation period, the cytotoxicity was measured

using SRB assay as described earlier. Morphological changes were evaluated using a phase contrast microscope.

2.7. Acridine orange/Ethidium bromide (AO/EB) staining

To evaluate if *p*CA has a protective effect on Dox induced apoptosis, a fluorescent double-staining method involving AO/EB was employed. H9c2 cells (8×10^4 cells/well in 24-well plates) were seeded in DMEM medium and incubated for 48 h at 37 °C with 95% air and 5% CO_2 to allow the cells to become semi-confluent. After this period the cells were pre/co-treated with *p*CA (380 μM) and Dox (1.5 Dox μM) respectively, for 24 h. After 24 h, adhered cells were rinsed in PBS (pH 7.4) and a 1:1 solution of AO (100 μg/ml)/EB (100 μg/ml) was added to the treated wells. The plates were incubated in the dark at 37 °C for 30 min. Each well was examined under a fluorescence microscope with a FITC filter at 20× magnification to determine the live and dead cells [21].

2.8. DAPI staining

DAPI staining was done to detect the changes in nuclear morphology and DNA damage during treatment with *p*CA and Dox. H9c2 cells (8×10^4 cells/well in 24-well plates) were seeded in DMEM medium and incubated for 48 h at 37 °C with 95% air and 5% CO_2 to allow the cells to become semi-confluent. Semi confluent cells were then pre/co-administered with *p*CA (380 μM) and Dox (1.5 Dox μM) respectively, for 24 h. Following the treatment period, adherent cells were rinsed thrice in PBS to completely remove traces of the growth medium. Cells were then fixed for 10 min in 3.7% formaldehyde and again rinsed thrice in PBS prior to permeabilisation in 0.2% Triton-X-100 for 5 min. Cells were then washed and incubated with DAPI labelling solution for 5 min in the dark. The labelling solution was then aspirated off and stained cells were rinsed thrice in PBS and changes in the nuclear morphology and DNA damage was observed using a fluorescence microscope (Olympus) with the DAPI filter at 20× magnification [22].

2.9. DCFH-DA staining

Intracellular ROS levels were measured using a cell permeable fluorescent probe 2′,7′-dichlorofluorescin diacetate (DCFH-DA). DCFH-DA diffuses through the cell membrane where it is hydrolysed by an intracellular esterase to the non-fluorescent dichlorofluorescin (DCFH) which is rapidly oxidised by ROS to fluorescent dichlorofluoresin. H9c2 cells (8×10^4 cells/well in 24-well plates) were seeded in DMEM medium and incubated for 48 h at 37 °C with 95% air and 5% CO_2 to allow the cells to become semi-confluent. Semi-confluent H9c2 cells were treated with *p*CA (380 μM) and Dox (1.5 Dox μM) for 6 h. After the treatment period, DCFH-DA (in absolute DMSO) was added to treated plates at a final concentration of 10 μM and incubated in the dark at 37 °C for 30 min. Post-staining, plates were rinsed twice with PBS and images were taken on a fluorescent microscope (Olympus) using the appropriate bandpass FITC filter and relative fluorescence was measured using ImageJ 1.48 software [23].

2.10. Determination of mitochondrial membrane potential (MMP; $\Delta\psi m$)

To determine the effect of *p*CA on the electrical potential across the inner mitochondrial membrane of Dox treated H9c2 cells, Rhodamine 123 (R-123), a lipophilic,cationic indicator was used. H9c2 cells (2×10^4 cells/well in 96-well plates) were seeded in DMEM medium and incubated for 48-hours at 37 °C with 95% air and 5% CO_2 to allow the cells to become semi- confluent. After this period cells were pre/co-administered with *p*CA (380 μM) and Dox (1.5 μM Dox) respectively, for 24 h. Cells were then rinsed with PBS and fresh media containing R-123 solution (10 μg/ml) was added to treated wells and the plates were incubated in the dark at 37 °C for 20–30 min. Subsequently, the cells were washed twice with PBS and the cell images were taken using a fluorescence microscope (Olympus 1 × 51) [24].

2.11. Measurement of the intracellular calcium levels

Alterations in intracellular calcium levels were evaluated using the ratiometric probe FURA-2-AM. H9c2 cells (2×10^4 cells/well) were pre/co-treated with *p*CA (380 μM) and Dox (1.5 μM Dox) respectively, for 24 h. After the treatment period, culture medium in the wells was replaced with Krebs buffer (1 mM $CaCl_2$; 132 mM NaCl; 4 mM KCl; 1.2 mM Na_2HPO_4; 1.4 mM $MgCl_2$; 6 mM Glucose; 10 mM HEPES, pH 7.4), supplemented with 1 mg/ml bovine serum albumin (BSA) and 5 μM FURA-2AM, and incubated at 37 °C in the dark for 40 min. Cells were rinsed twice with Kreb's buffer following the incubation period and fresh buffer supplemented with BSA minus the probe was added to the wells. The cells were then observed by fluorescence microscopy using the appropriate bandpass filter. (Olympus 1 × 51) [25].

2.12. Statistical analysis

Experimental results are expressed as mean ± S.D of three independent experiments. One-way ANOVA using SPSS-19,IBM Technologies Software was used for statistical analysis, followed by Duncan's multiple comparison test to assess the significance between groups. Value of $p < 0.05$ was considered to be statistically significant.

3. Results

3.1. Radical scavenging activity of pCA

The total antioxidant capacity of different concentrations of *p*CA was calculated from the decolourisation of $ABTS^{*+}$, which was measured spectrophotometrically at 734 nm. Interactions of the dye with *p*CA reduced the absorbance values of the radical cation and the results obtained have been expressed as percentage inhibition in comparison to the controls. The results showed *p*CA to have strong ABTS radical scavenging activity in a concentration dependent manner (Fig. 2A). Fig. 2B shows the FRAP activity for different concentrations of *p*CA. FRAP assay is a simple inexpensive method to evaluate the total antioxidant potential of plant components. Higher the FRAP value obtained, greater is the antioxidant power of the compound. Our results showed that FRAP activity increased with higher concentrations of *p*CA. Concentrations of *p*CA from 0.04–9.5 μM showed a lower FRAP activity; while 38.1 μM and 152 μM showed a higher antioxidant potential. The aforementioned concentrations (38.1 and 152 μM) also showed a 100% ABTS scavenging activity when tested.

3.2. Cell viability after exposure to different concentrations of Dox and pCA alone

The viability of H9c2 cardiomyoblast cells was evaluated after 72 h of exposure to different concentrations of DOX and *p*CA by SRB method. As shown in Fig. 3A, Dox treatment induced significant cytotoxicity in a dose dependent manner. The IC_{50} value was found to be 1.5 μM. This concentration was found to be ideal through initial AO/EB staining and was set as the working drug concentration for all further experiments related to drug studies. We examined the effect of different concentrations of *p*CA on H9c2 cell viability to select a concentration of *p*CA which is both non-toxic to cells as

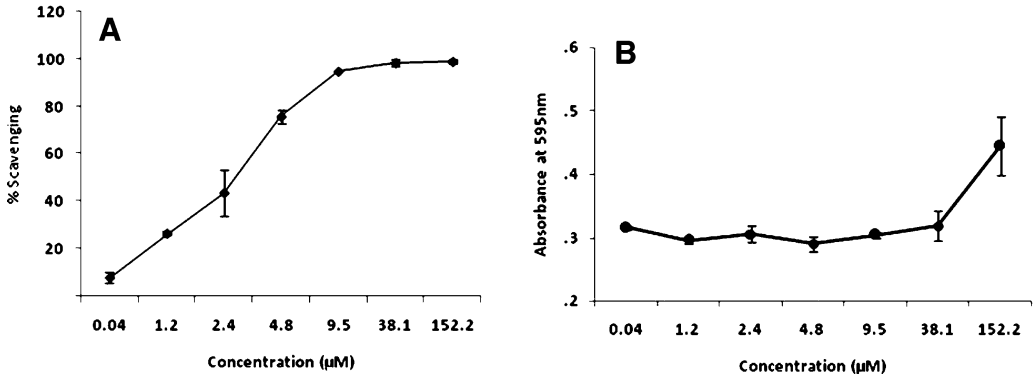

Fig. 2. Graphical presentation on the effect of different concentrations of *p*CA on *in vitro* ABTS scavenging and FRAP activity. (A) ABTS scavenging activity, (B) FRAP activity. The values are expressed as ±S.D. of three separate experiments.

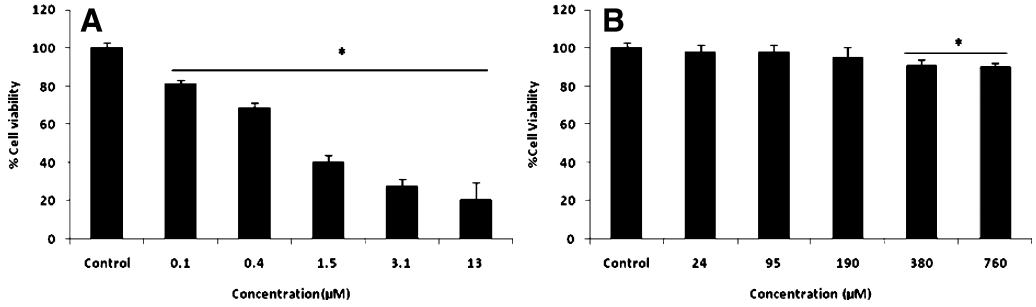

Fig. 3. Cytotoxic effect of different concentrations of Dox and *p*CA against H9c2 cells. Values are expressed as ±SD of three individual experiments. (A) Different concentrations of Dox; (B) different concentrations of *p*CA. *Significant compared to control ($p < 0.05$).

well as effective in preventing/improving Dox induced cytotoxicity. The cells were incubated with *p*CA at different concentrations (23–760 μM) for 72 h. The percentage of cell viability under different treatment conditions has been shown in Fig. 3B. The results clearly showed that *p*CA was not cytotoxic towards the relevant cell line at tested concentrations. 380 μM and 761 μM *p*CA displayed a lower range of cytotoxicity, which was not prominent in comparison to Dox treatment. Since the cytotoxicity was at a negligibly lower range, the concentration—380 μM, with higher free radical scavenging activity (results not shown) was used for the further studies in conjunction with Dox.

3.3. p*CA reduces Dox induced cytotoxicity*

Fig. 4 shows the effect of pre-treatment and co-administration of *p*CA on Dox induced cytotoxicity in H9c2 cell lines. Dox treatment at a concentration of 1.5 μM showed significant cytotoxicity. The cell viability was found to be 43% after 72 h. The results shown indicate that both pre and co-administration of *p*CA significantly reduced the cell toxicity induced by Dox. Pre-treatment of *p*CA helped to retain 86% cell viability and co-administration of *p*CA helped to retain the cell viability at 84% (Fig. 4, panel F). Morphological analysis showed that Dox treatment induced severe structural changes to H9c2 cells. Most of the cells appeared to be rounded off, losing their adherent property following drug treatment. (Fig. 4, panel B). Treatment of cells with *p*CA did not show any significant structural changes/damages to the regular cell morphology (Fig. 4, panel C). Both pre and co-administration of *p*CA prevented the structural changes induced by Dox on H9c2 cells (Fig. 4, panels D,E).

3.4. p*CA inhibits Dox induced apoptosis in H9c2 cells*

Since Dox decreased cell viability and affected cell size, it was hypothesised that apoptosis might be involved in the reduction of cell viability induced by Dox. When the treated and control cells were stained with the DNA-binding dye DAPI, the cell morphology of treated cells revealed nuclei with condensed chromatin and fragmented nuclei, which are characteristics of apoptotic cells (Fig. 5, panel G). When the H9c2 cells were exposed to 1.5 μM Dox for 24 h, the total number of viable cells and the size of most cells reduced noticeably. Shrunken/swollen cytoplasm and nuclei pyknosis could also be observed. Pre treatment and co-administration of *p*CA showed significant reduction in these properties induced by Dox (Fig. 5, panels I,J). AO/EB staining revealed that exposure to 1.5 μM Dox reduced the viability of the cells and the stained cells appeared to be red in colour, characteristic of non-viable cells. (Fig. 5, panel B). Treatment with *p*CA did not show any red coloured cells which is indicative of the non-cytotoxic nature of the compound (Fig. 5, panel C). Pre treatment and co-administration of *p*CA showed significant reduction in the numbers of non-viable compared to the cells treated with 1.5 μM Dox alone (Fig. 5, panels D,E).

3.5. p*CA modulates ROS production in H9c2 cells*

Fig. 6 shows the effect of ROS production in Dox and *p*CA treated cells. Treatment with 1.5 μM Dox showed significant increase in ROS production as indicated by a 2-fold increase in DCF fluorescence (Fig. 6, panels C,F). Cells treated with *p*CA alone showed DCF fluorescence at normal levels (Fig. 6, panels C,F). Cells pretreated and/ cotreated with *p*CA followed by Dox showed a significant reduction in ROS production as evident from a 1.3 and 1.5 fold reduction in DCF fluorescence as compared to cells treated with Dox alone (Fig. 6, panels D–F).

3.6. p*CA modulates MMP in H9c2 cells exposed to Dox*

Fig. 7 shows the variations in mitochondrial membrane potential in Dox and *p*CA treated cells. Treatment with 1.5 μM Dox

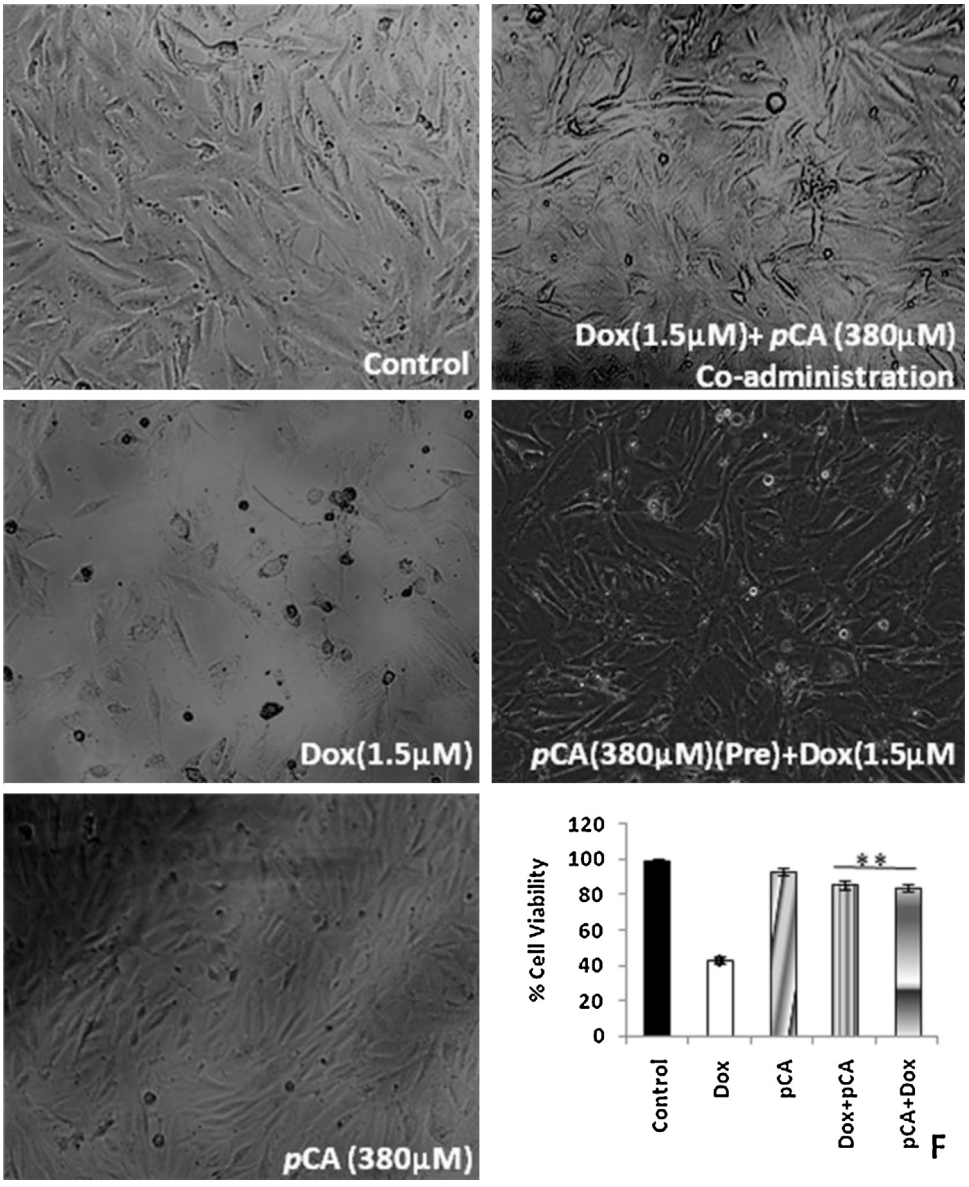

Fig. 4. Cytotoxic effect of pre and co-administration of *p*CA and Dox on H9c2 cells. Values are expressed as ±SD of three individual experiments. Typical morphological changes of H9c2 cells treated *p*CA, dox and pre/co-administration of *p*CA after 72 h of treatment. *F* indicates the % cell viability of control, Dox and *p*CA treated cells, Dox + *p*CA indicates co administration, *p*CA + Dox indicates pre treatment. *Significant compared to control ($p < 0.05$), **significant compared to Dox ($p < 0.05$). The picture is the representation of three separate experiments.

showed a significant decrease in MMP as indicated by significant reduction in R-123 fluorescence as shown (panel B). Cells treated with *p*CA alone showed a normal MMP (panel C). Pre and co-administration of *p*CA showed a significant restoration of MMP as evident from the higher fluorescence in comparison to exclusively Dox treated cells (panels D,E).

3.7. p*CA modulates intra cellular* Ca^{2+} *production in Dox treated H9c2 cells*

Fig. 8 shows the effects of treatment with Dox and *p*CA intracellular Ca^{2+} levels in cells. Treatment with 1.5 μM Dox showed a significant increase in Ca^{2+} production as indicated by increase in fluorescence within cells (panel B). Cells treated with *p*CA alone displayed fluorescence at levels identical to the control cells (panels C and A). Pre and co-administration of *p*CA showed a significant mobilisation of intracellular Ca^{2+} as evident from the lower fluorescence when compared to cells treated with Dox alone (panels D and E).

4. Discussion

Doxorubicin (Dox) is a powerful and effective drug used to treat a multitude of human neoplasm's including solid tumours. Though the drug is highly sought after for its remarkable anti-cancer effects, its clinical use is limited by severe cardiotoxic side effects. There are several mechanisms proposed for the cardiotoxic effects of Dox of which one major mechanism behind drug toxicity has been proved to be the excessive generation of ROS. The quinone moiety of Dox is converted enzymatically or non-enzymatically by cytochrome P_{450} into its semiquinone form by the acquisition of one electron. This semiquinone form is then oxidised by molecular oxygen to yield Dox (recycling) in its quinone form with a concomitant production of superoxide radicals [26]. Generated radicals are either scavenged by the dismutase enzymes spontaneously or at a slower rate

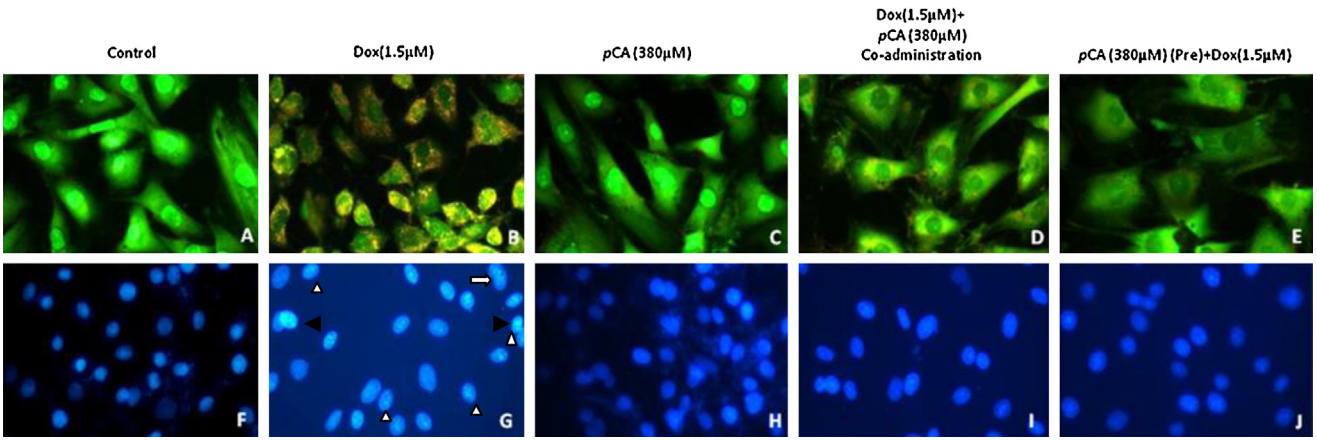

Fig. 5. Apoptotic analysis using AO/EB and DAPI staining on H9c2 cells treated pCA, dox and pre/co-administration of pCA after 24 h of treatment. The images were taken using fluorescent microscope (magnification 20×). (A) Control, (B) Dox (1.5 μM), (C) *p*CA (380 μM), (D) *p*CA (380 μM) + Dox (1.5 μM) co-administration. (E) Pre *p*CA (380 μM) + Dox (1.5 μM). The picture is the representation of three separate experiments. H9c2 cells treated with doxorubicin displaying morphological changes such as fragmented nuclei (white solid arrow heads), pyknosis/condensed chromatin (black solid arrow heads) and distorted nuclei of varying nuclear shape and size (white arrows) in comparison to the control/*p*CA treated cells.

producing H_2O_2 leading to cardiac toxicity [27]. Free radicals are generated continuously in the human body due to metabolism and diseases [28]. Oxidative damage, which causes extensive damage to tissues and biomolecules leading to various disease conditions, can be overcome using many synthetic drugs which are associated with severe adverse side effects. An alternative suggestion would require one to consume natural antioxidants from food and traditional medicine [29,30].

Due to the importance of Dox in chemotherapy, researchers around the world have put in great efforts to reduce its toxic side effects. The commonly employed strategies involve the use of drug analogues or combination therapy, which has proved to be unfruitful [31]. Presently, studies are progressing in a manner so as to isolate low toxic components from natural sources, which posses a significant free radical scavenging activity, that can be used along with Dox to prevent the severity of cardiotoxicity. *p*-coumaric acid (*p*CA), is a phenolic acid widely distributed in plants and one which forms an important constituent of the human diet worldwide [32]. Phenolic acids are capable of binding metal ions, scavenging reactive oxygen species (ROS), reactive nitrogen species (RNS), upregulating the endogenous antioxidant systems and preventing the oxidative damages to biomolecules [33]. Though previous studies showed that *p*CA alone or in combination with other natural products can modulate the lipid peroxidation levels in Dox treated rats [34,35], the effect of *p*CA on cardiomyoblasts have not been studied yet. This study was designed to evaluate the effect of *p*CA on H9c2 cardiomyoblast in *in vitro* conditions.

It was found that different concentrations of Dox (0.1–13 μM) showed a significant cytotoxicity on cardiomyoblasts in a dose dependent manner (Fig. 3), while different concentrations of *p*CA (24-760 μM) did not show cytotoxicity towards H9c2 cells. We determined the ideal concentration of *p*CA as 380 μM and that of Dox as 1.5 μM to study the protective effect of *p*CA on Dox treated cells. Dox treatment is more toxic to undifferentiated muscle cells, contributing to impaired cardiac development and toxicity persistence. H9c2 myoblasts, a rat embryonic cell line, which has the ability to differentiate into a skeletal or cardiac muscle phenotype, can be instrumental in understanding DOX cytotoxicity [36].

To determine the effect of Dox and *p*CA on H9c2 morphology, cells were treated with Dox (1.5 μM) and *p*CA (380 μM) for 72 h and photographs were taken using a phase contrast microscope (Fig. 4). The data showed that cell density was significantly decreased on Dox treatment with concomitant loss of their adherent nature and appeared to be rounded indicating progressive cell death. While cells pre/co-administered with Dox and *p*CA showed significant cell density with normal morphology. Previous studies showed that H9c2 cell when exposed to lower concentrations of Dox causes alterations in fibrous structural proteins including the nuclear lamina and sarcomeric cardiac myosin, as well as mitochondrial depolarisation and fragmentation, membrane blebbing with cell shape changes, and phosphatidylserine externalisation. At higher concentrations, more profound alterations are evident, including nuclear swelling with disruption of nuclear membrane structure, mitochondrial swelling, and extensive cytoplasm vacuolisation [37].

The cell lines treated with Dox and *p*CA was also stained with AO/EB and DAPI to determine the apoptotic effect. Results clearly showed that the cells treated with Dox undergo loss of cell viability as indicated by the presence of a large amount of red coloured cells in comparison to the control. Cells pre/co-administered with Dox and *p*CA showed significant reduction in dying cells as indicated by the lower number of red coloured cells. There are numerous evidences suggesting that cardio myocytes undergo apoptosis following Dox treatment both *in vivo* and *in vitro*, indicating that apoptosis is the main mechanism leading to Dox mediated cardiac dysfunction [38,39]. It was earlier reported that *p*CA, through its strong antioxidant character exerts a protective effect on the alterations in gene-expression profile in sodium arsenite induced cardiotoxicity in rats [40]. *p*CA also protected isoproterenol induced myocardial apoptosis by inhibiting oxidative stress in Wistar rats. The protective effects of *p*CA as observed in the previous studies were attributed to its anti-lipid peroxidative, anti- apoptotic and antioxidant properties. *p*CA also increased the myocardial expression of Bax, caspase-8, caspase-9 and Fas genes and showed a decrease in the myocardial expression of Bcl-2 and Bcl-xL genes [41].

To evaluate whether the protective effect of *p*CA is dependent on the reduction of ROS in mitochondria, the cells were stained with DCFH-DA after 6 h of treatment. The results showed that Dox treatment significantly induced ROS formation in cells as evidenced from the higher fluorescent intensity, while cells treated with *p*CA in the pre and co-administration mode with Dox showed reduced levels of ROS levels in comparison to the Dox treated cells. *p*CA significantly reduced the ROS formation in H9c2 cells, which may be partly due to the ability of *p*CA to quench the free radicals initiated by Dox. Dox induces an iron-mediated increase in ROS and cellular damage by futile redox cycling [42]. This redox cycle in the presence of heavy metals, such as iron leads to the formation of superoxide,

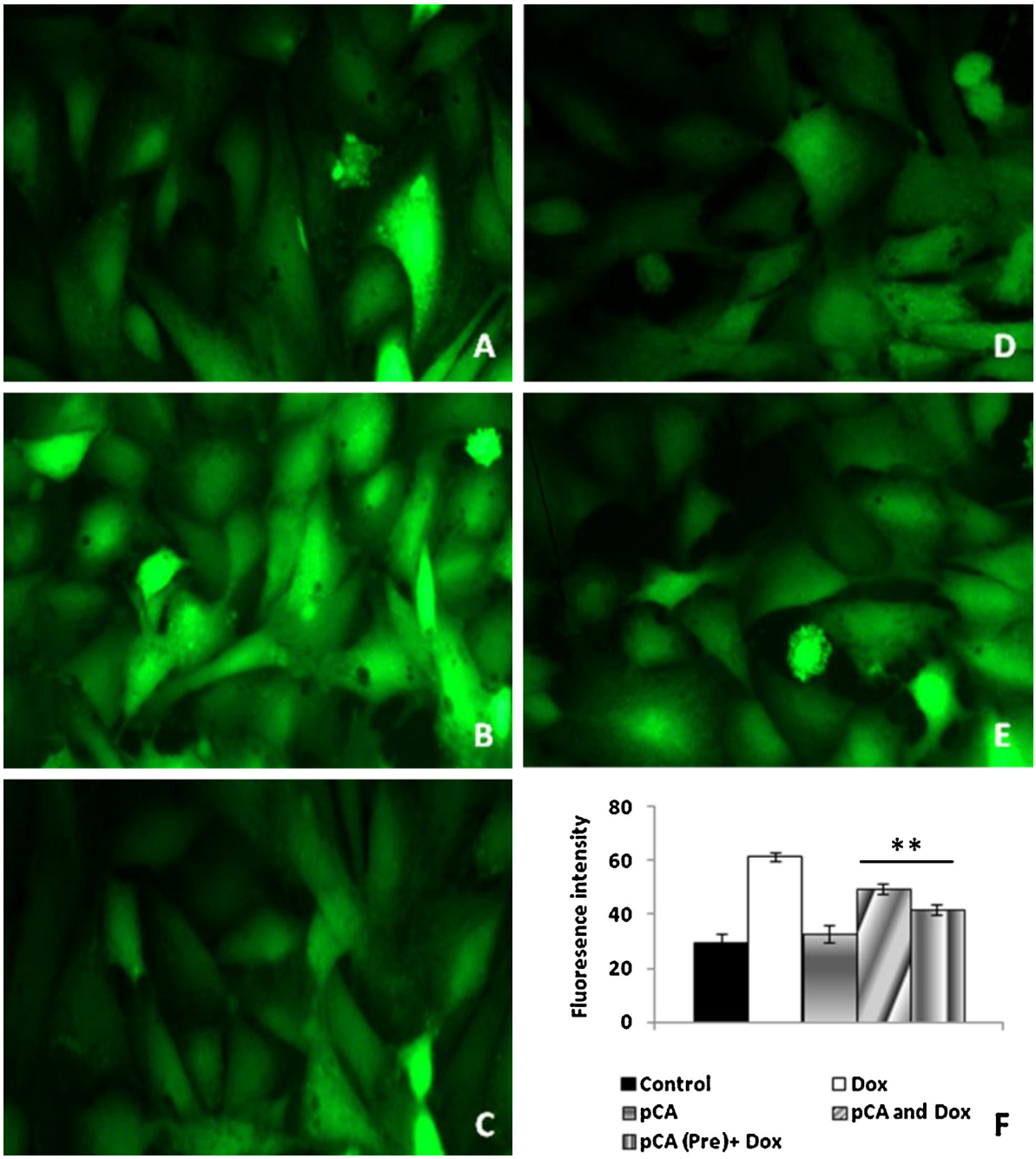

Fig. 6. Analysis of ROS formation using DCFH-DA staining on H9c2 cells treated *p*CA, dox and pre/co-administration of *p*CA after 6 h of treatment. The images were taken using light (magnification 20×). (A) Control, (B) Dox (1.5 μM) (C) *p*CA (380 μM), (D) *p*CA (380 μM) + Dox (1.5 μM) co-administration, (E) pre *p*CA(380 μM) + Dox (1.5 μM). The picture is the representation of three separate experiments. *F* shows the mean fluorescent intensity of control and treated groups. *Significant compared to control ($p < 0.05$), **significant compared to Dox ($p < 0.05$), #significant compared to pCA and Dox ($p < 0.05$).

which is converted to H_2O_2 spontaneously or by superoxide dismutase. Subsequently, H_2O_2 may be converted to highly toxic hydroxyl radicals leading to cardiomyopathy [43–45].

The molecular mechanisms of doxorubicin induced mitochondrial injury in cardiac muscle cells are largely unclear [46]. Dox causes DNA damage and formation of reactive oxygen species, eventually resulting in apoptosis. The dissipation of membrane potential ($\Delta\psi$) is one of the markers for mitochondrial involvement in apoptosis [47]. In the present study, we set up Rhodamine-123 staining experiment to assess the therapeutic potential of *p*CA in preventing the dissipation of $\Delta\psi$ in doxorubicin-induced apoptosis in H9c2 cells. It was found that *p*CA prevented the reduction of $\Delta\psi$ when pre/co administered with Dox.

Dox-induced cardiotoxicity is also characterised by an increase in intracellular calcium levels. Dysregulation of intracellular calcium concentrations is both a result and a cause of ROS-generation [48]. The ROS and H_2O_2 generated by these mechanisms alter normal calcium homeostasis in a variety of muscle cell types via disruption of normal sarcoplasmic reticulum function [49]. The decrease in ROS production and intracellular calcium levels in *p*CA treated H9c2 cells indicate that the protective effect of this compound is mediated through mitochondria.

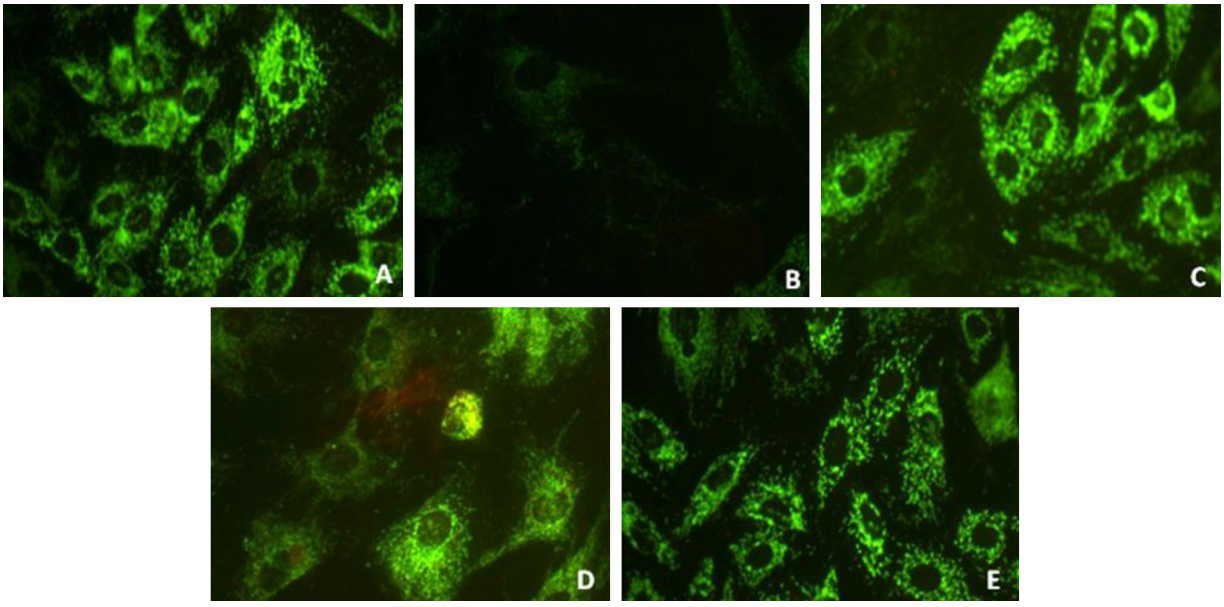

Fig. 7. Analysis of mitochondrial membrane potential using rhodamine 123 in H9c2 cells treated *p*CA, dox and pre/co-administration of *p*CA after 24 h of treatment. The images were taken using light (magnification 20×). (A) Control, (B) Dox (1.5 μM) (C) *p*CA (380 μM), (D) *p*CA (380 μM) + Dox (1.5 μM) co administration, (E) pre treatment of *p*CA (380 μM) + Dox (1.5 μM). The picture is the representation of three separate experiments.

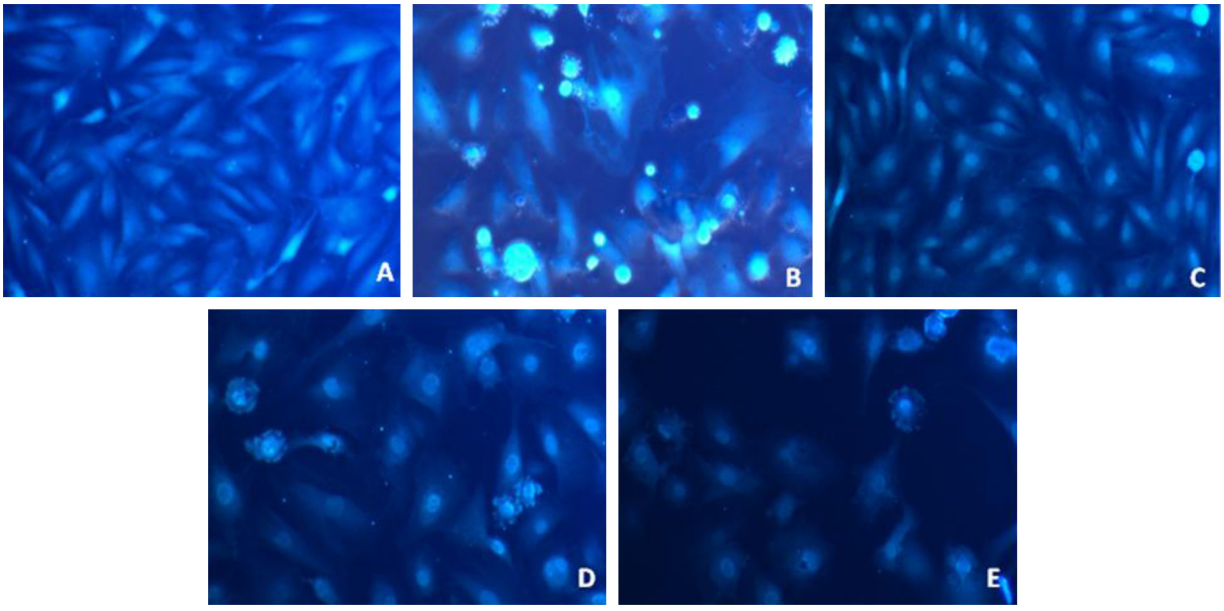

Fig. 8. Intracellular calcium analysis levels determined using FURA-2/AM in H9c2 cells treated *p*CA, dox and pre/co-administration of *p*CA after 24 h of treatment. The images were taken using fluourescent microscope (magnification 20×). (A) Control, (B) Dox (1.5 μM) (C) *p*CA (380 μM), (D) *p*CA (380 μM) + Dox (1.5 μM) co-administration, (E) pre treatment of *p*CA (380 μM) + Dox (1.5 μM). The picture is the representation of three separate experiments.

Results from the present study suggest that *p*CA is capable of reducing the toxic effect induced by Dox in H9c2 cell lines, which may be due to the reduced drug metabolism, down regulation of pro-apoptotic molecules as well as reduction in oxidative stress by preventing ROS formation mediated through the inhibition of Fe-Dox complex formation. Further work at proteomic and genomic levels could give one more insight into the precise molecular targets by which *p*CA exerts its protective effects on Dox induced toxicity.

5. Conclusion

In summary, this study provides evidence showing that Dox induced cardiomyoblast toxicity is partly mediated by mitochondrial ROS production. *p*CA, with its potent antioxidant potential, attenuates ROS-induced cardiomyoblast damage when pre-treated or co-treated with Dox.

Conflict of interest

The authors declare that there is no conflict of interest.

Acknowledgement

The authors are grateful to School of Biosciences, Mahatma Gandhi University and Department of Biotechnology, Government of India for the excellent research facilities supported through the

DBT-MSUB-IPLS (BUILDER) programme. Junior research fellowship (JRF) from DBT-MSUB-IPLS to MCS is deeply acknowledged.

References

[1] J. Das, J.P. Ghosh, P.C.S. Manna, Taurine suppresses doxorubicin-triggered oxidative stress and cardiac apoptosis in rat via up-regulation of PI3-K/Akt and inhibition of p53, p38-JNK, Biochem. Pharmacol. 81 (2011) 891–909.
[2] P. Menna, E. Salvatorelli, G. Minotti, Doxorubicin degradation in cardiomyocytes, J. Pharmacol. Exp. Ther. 322 (2007) 408–419.
[3] S.R. Umansky, J.P. Shapiro, G.M. Cuenco, M.W. Foehr, I.C. Bathurst, L.D. Tomei, Prevention of rat neonatal cardiomyocyte apoptosis induced by simulated in vitro ischemia and reperfusion, Cell Death Differ. 4 (1997) 608–616.
[4] H.M. Olson, D.M. Young, D.J. Prieur, A.F. LeRoy, R.L. Reagan, Electrolyte and morphologic alteration of myocardium in adriamycin-treated rabbits, Am. J. Pathol. 77 (1974) 439–454.
[5] C.E. Myers, L. Gianni, C.B. Simone, R. Klecker, R. Greene, Oxidative destruction of erythrocyte ghost membranes catalyzed by the doxorubicin–iron complex, Biochemistry 21 (1982) 1707–1712.
[6] R.D. Olson, P.S. Mushlin, Doxorubicin cardiotoxicity: analysis of prevailing hypotheses, FASEB J. 4 (1990) 3076–3086.
[7] A. Piasek, A. Bartoszek, J. Namieśnik, Phytochemicals that counteract the cardiotoxic side effects of cancer chemotherapy, Postepy Hig. Med. Dosw. (Online) 163 (2009) 142–158.
[8] Q. Dong, L. Chen, Q. Lu, S. Sharma, L. Li, S. Morimoto, G. Wang, Quercetin attenuates doxorubicin cardiotoxicity by modulating Bmi-1 expression, Br. J. Pharmacol. 171 (2014) 4440–4454.
[9] S. Subburaman, K. Ganesan, M. Ramachandran, Protective role of naringenin against doxorubicin-induced cardiotoxicity in a rat model: histopathology and mRNA expression profile studies, J. Environ. Pathol. Toxicol. Oncol. 33 (2014) 363–376.
[10] J. Zheng, H.C. Lee, M.M. Bin Sattar, Y. Huang, J.S. Bian, Cardioprotective effects of epigallocatechin-3-gallate against doxorubicin-induced cardiomyocyte injury, Eur. J. Pharmacol. 652 (2011) 82–88.
[11] J.R. Walker, A. Sharma, M. Lytwyn, S. Bohonis, J. Thliveris, P.K. Singal, D.S. Jassal, The cardioprotective role of probucol against anthracycline and trastuzumab-mediated cardiotoxicity, J. Am. Soc. Echocardiogr. 24 (2011) 699–705.
[12] E.D. Danz, J. Skramsted, N. Henry, J.A. Bennett, R.S. Keller, Resveratrol prevents doxorubicin cardiotoxicity through mitochondrial stabilization and the Sirt1 pathway, Free Radic. Biol. Med. 46 (2009) 1589–1597.
[13] W. Mao, M.A. Schuler, M.R. Berenbaum, Honey constituents up-regulate detoxification and immunity genes in the western honey bee *Apis mellifera*, Proc. Natl. Acad. Sci. U. S. A. 110 (2013) 8842–8846.
[14] Z. Quinde-Axtell, B.K. Baik, Phenolic compounds of barley grain and their implication in food product discoloration, J. Agric. Food. Chem. 54 (2006) 9978–9984.
[15] G.M. Carrero, C.G. García, J.A. Pérez-Bustamante, Analysis of polyphenolic compounds of different vinegar samples, Z. Lebensm. Unters. Forsch. 199 (1994) 29–31.
[16] L.R. Ferguson, Z. Shuo-tun, P.J. Harris, Antioxidant and antigenotoxic effects of plant cell wall hydroxycinnamic acids in cultured HT-29, Mol. Nutr. Food. Res. 49 (2005) 585–693.
[17] K. Kikugawa, T. Hakamada, M. Hasunuma, T. Kurechi, Reaction of *p*-hydroxycinnamic acid derivatives with nitrite and its relevance to nitrosamine formation, J. Agric. Food. Chem. 1 (1983) 780–785.
[18] R. Re, N. Pellegrini, A. Proteggente, A. Pannala, A. Pannala, M. Yang, C. Rice-Evans, Antioxidant activity applying an improved ABTS radical cation decolorization assay, Free Radic. Biol. Med. 26 (1999) 1231–1237.
[19] I.F. Benzie, J.J. Strain, The ferric reducing ability of plasma (FRAP) as a measure of antioxidant power: the FRAP assay, Anal. Biochem. 239 (1996) 70–76.
[20] S.P. Fricker, The application of sulforhodamine B as a colorimetric endpoint in a cytotoxicity assay, Toxicol. In Vitro 8 (1994) 821–822.
[21] D. Baskić, S. Popović, P. Ristić, N.N. Arsenijević, Analysis of cyclohexamide induced apoptosis in human leukocytes: Fluorescence microscopy using annexinV/propidium iodide *versus* acridine orange or ethidium bromide, Cell Biol. Int. 30 (2006) 924–932.
[22] B. Chazotte, Mounting live s onto microscope slides, Cold Spring Harb. Protoc. 1 (2011) 1–4.
[23] F. Warleta, C. Sanchez Quesada, M. Campos, Y. Allouche, G. Beltran, J.J. Gaforio, Hydroxytyrosol protects against oxidative DNA damage in human breast cells, Nutrients 3 (2011) 839–857.
[24] Y. Wang, X. Zhao, X. Gao, XXN, Y.Y. ie, X.F. ang, an, Development of fluorescence imaging-based assay for screening cardioprotective compounds from medicinal plants, Anal. Chim. Acta 702 (2011) 87–94.
[25] J.R. Wu, S.F. Liou, S.W. Lin, C.Y. Chai, Z.K. Dai, J.C. Liang, I.J. Chen, J.L. Yeh, Lercanidipine inhibits vascular smooth muscle cell proliferation and neointimal formation via reducing intracellular reactive oxygen species and inactivating Ras-ERK1/2 signaling, Pharmacol. Res. 59 (2009) 48–56.
[26] A.R. Goeptar, J.M. Te Koppele, E.K. Lamme, J.M. Piqueí, N.P.E. Vermeulen, Cytochrome P450 2B1-mediated one-electron reduction of adriamycin: a study with rat liver microsomes and purified enzymes, Mol. Pharmacol. 44 (1993) 1267–1277.
[27] A. Bast, G.R.M.M. Haenen, A.M.E. Bruynzeel, W.J.F. Van der Vijgh, Protection by flavonoids against anthracycline cardiotoxicity: from chemistry to clinical trials, Cardiovasc. Toxicol. 7 (2007) 154–159.
[28] K.J. Yeum, G. Aldini, H.Y. Chung, N.I. Krinsky, R.M. Russell, The activities of antioxidant nutrients in human plasma depend on the localization of attacking radical species, J. Nutr. 133 (2003) 2688–2691.
[29] A. Jerome-Morais, A.M. Diamond, M.E. Wright, Dietary supplements and human health: for better or for worse? Mol. Nutr. Food Res. 55 (2011) 122–135.
[30] G. Bjelakovic, C. Gluud, Surviving antioxidant supplements, J. Natl. Can. Inst. 99 (2007) 742–743.
[31] G. Khan, S.E. Haque, T. Anwer, M.N. Ahsan, M.M. Safhi, M.F. Alam, Cardioprotective effect of green tea extract on doxorubicin induced cardiotoxicity in rats, Acta Pol. Pharm. 71 (2014) 861–868.
[32] A. Scalbert, G. Williamson, Dietary intake and bioavailability of polyphenols, J. Nutr. 130 (2000) 2073S–2085S.
[33] F. Ursini, F. Tubaro, J. Rong, A. Sevanian, Optimization of nutrition: polyphenols and vascular protection, Nutr. Rev. 57 (1999) 241–249.
[34] S.S. Shiromwar, V.R. Chidrawar, Combined effects of p-coumaric acid and naringenin against doxorubicin-induced cardiotoxicity in rats, Pharmacognosy Res. 3 (2011) 214–219.
[35] M.H. Abdel-Wahab, M.A. El-Mahdy, M.F. Abd-Ellah, G.K. Helal, F. Khalifa, F.M. Hamada, Influence of *p*-coumaric acid on doxorubicin-induced oxidative stress in rat's heart, Pharmacol. Res. 48 (2003) 461–465.
[36] A.F. Branco, SF, A.C.M. Sampaio, J.H. oreira, K.B.W. oly, I. allace, P.J.O. Baldeiras, V.A.S. liveira, ardao, Differentiation-dependent Ddoxorubicin toxicity on H9c2 cardiomyoblasts, Cardiovasc. Toxicol. 12 (2012) 326–340.
[37] V.A. Sardão, P.J. Oliveira, J. Holy, C.R. Oliveira, K.B. Wallace, Morphological alterations induced by doxorubicin on H9c2 myoblasts: nuclear, mitochondrial, and cytoskeletal targets, Cell Biol. Toxicol. 25 (2009) 227–243.
[38] S. Arunachalam, S.Y. Kim, S.H. Lee, Y.H. Lee, M.S. Kim, B.S. Yun, H.K. Yi, P.H. Hwang, Davallialactone protects against adriamycin-induced cardiotoxicity in vitro and in vivo, J. Nat. Med. 66 (2012) 149–157.
[39] D. Kumar, L.A. Kirshenbaum, T. Li, I. Danelisen, P.K. Singal, Apoptosis in adriamycin cardiomyopathy and its modulation by probucol, Antioxid. Redox Signal. 3 (2001) 135–145.
[40] N. Prasanna, M. Rasool, Modulation of gene-expression profiles associated with sodium arsenite-induced cardiotoxicity by *p*-coumaric acid, a common dietary polyphenol, J. Biochem. Mol. Toxicol. 28 (2014) 174–180.
[41] P. Stanely Mainzen Prince, A.J. Roy, *p*-Coumaric acid attenuates apoptosis in isoproterenol-induced myocardial infarcted rats by inhibiting oxidative stress, Int. J. Cardiol. 168 (2013) 3259–3266.
[42] J.M. Berthiaume, K.B. Wallace, Adriamycin-induced oxidative mitochondrial cardiotoxicity, Cell. Biol. Toxicol. 23 (2007) 15–25.
[43] Y. Ichikawa, M. Ghanefar, M. Bayeva, R. Wu, A. Khechaduri, S.V. Naga Prasad, R.K. Mutharasan, T.J. Naik, H. Ardehali, Cardiotoxicity of doxorubicin is mediated through mitochondrial iron accumulation, J. Clin. Invest. 124 (2014) 617–630.
[44] G.S. Panjrath, V. Patel, C.I. Valdiviezo, N. Narula, J. Narula, D. Jain, Potentiation of doxorubicin cardiotoxicity by iron loading in a rodent model, J. Am. Coll. Cardiol. 49 (2007) 2457–2464.
[45] C.E. Myers, W.P. McGuire, R.H. Liss, I. Ifrim, K. Grotzinger, R.C. Young, Adriamycin: the role of lipid peroxidation in cardiac toxicity and tumor response, Science 197 (1977) 165–167.
[46] L. Gille, H. Nohl, Analyses of the molecular mechanism of adriamycin-induced cardiotoxicity, Free Radic. Biol. Med. 23 (1997) 775–782.
[47] M. Huigsloot, I.B. Tijdens, G.J. Mulder, B. Water, Differential regulation of doxorubicin-induced mitochondrial dysfunction and apoptosis by Bcl-2 in mammary adenocarcinoma (MTLn3) cells, J. Biol. Chem. 277 (2002) 35869–35879.
[48] S.V. Kalivendi, E.A. Konorev, S. Cunningham, S.K. Vanamala, E.H. Kaji, J. Joseph, B.B. Kalyanaraman, Doxorubicin activates nuclear factor of activated T-lymphocytes and Fas ligand transcription: role of mitochondrial reactive oxygen species and calcium, Biochem. J. 389 (2005) 527–539.
[49] M. Arai, A. Yoguchi, T. Takizawa, T. Yokoyama, T. Kanda, M. Kurabayashi, R. Nagai, Mechanism of doxorubicin-induced inhibition of sarcoplasmic reticulum Ca(2+)-ATPase gene transcription, Circ. Res. 86 (2000) 8–14.